IOP Conf. Series: Materials Science and Engineering **966** (2020) 012042 doi:10.1088/1757-899X/966/1/012042

Simulation of patterns of crystallizing ingot macrostructure formation

O Yu Sidorov

Ural Federal University named after the First President of Russia B N Yeltsin, Nizhniy Tagil Technological Institute, 59, Krasnogvardeyskaya str, Nizhniy Tagil, 622000, Russia

E-mail: sidorov-ou-62@yandex.ru

Abstract. The electromagnetic, hydrodynamic, and temperature fields of a crystallizing cylindrical ingot with a diameter of 163 mm have been calculated using the finite-difference method. Crystallization has been simulated in an electromagnetic crystallizer. The crystallization rate has been calculated, and then the ingot areas have been divided into small crystals, dendrites and globular ones. Quantitatively, the relationship between the temperature field gradient during crystallization and the ingot structure can be expressed by the following rules: 1) elongated grains of about 10 mm – cooling rate of about $1.8 \cdot 10^{-4}$ kg/s; 2) elongated grains of about 20–30 mm – cooling rate of about $0.7 \cdot 10^{-4}$–$1.8 \cdot 10^{-4}$ kg/s; 3) globular grains with a size of 10–20 mm – cooling rate of less than $0.7 \cdot 10^{-4}$ kg/s. The possibility of simulation of the ingot structure during its crystallization based on the relationship between the crystallization rate and the grain size has been shown. The influence of the inductor current frequency on the structure of a crystallizing ingot has been simulated. It has been shown that an increase in the current frequency from 5 to 500 Hz leads to the expansion of the area with small crystals.

1. Introduction

A large number of papers have been devoted to experimental and theoretical studies of the electromagnetic field impact on metal systems. The electromagnetic field impact is expressed in grain refinement, leveling of the chemical composition with respect to the ingot volume [1]. In this case, the grain size can be related to the local cooling rate (see, for example, [2]).

It is noted in [3] that the electromagnetic field can change the temperature gradient, improve the coating microstructure, reduce cracks, and improve the coating microhardness. In the study [4], an assumption is made that growing dendrites are destroyed under the influence of a melt flow (under the influence of an electromagnetic field), and then some of the dendrite fragments are partially remelted. The possibility of concentration changes in the alloy composition under the influence of an electromagnetic field is shown in the papers [5, 6]. A change in the melt crystallization front under the influence of an electromagnetic field is shown in the paper [7], and the direction of growth of columnar crystals almost becomes parallel. The study [8, 10] provides data on the acceleration of purification of molten Al, Si from boron and phosphorus using a rotating electromagnetic field. It is noted in the paper [9] that the microstructure of Al-Zn-Mg-Cu alloy slabs was significantly improved by using an alternating magnetic field with industrial current frequency and frequency of 386 A and 50 Hz, respectively. The studies [11] for the aluminum alloy with silicon show the feasibility of electromagnetic impact during the assimilation of silicon in liquid aluminum. The feasibility of

electromagnetic stirring during continuous casting of large-size slabs is shown in the paper [12]. The study [13] considers the concentration non-uniformity of the composition in relation to electromagnetic stirring. For a more effective impact of the electromagnetic field on a liquid or crystallizing molten metal, various schemes of inductors and their power modes have been proposed (see, for example, [13–18]).

2. Problem statement

This study aims at the simulation of an ingot structure (grain size) during its crystallization in a traveling electromagnetic field for various inductor current frequencies. To solve this problem, it is necessary to use a comprehensive approach that takes into account processes of various physical and chemical nature and various time constants. In this case, electromagnetic processes can be considered as quasi-steady. The hydrodynamic characteristics (speed and pressure) shall be recalculated at each time interval. Thermal processes are considered in dynamics.

An electromagnetic crystallizer for casting a brass cylindrical billet with a diameter of about 160 mm was selected as the study object [19]. The inductor winding coils are made of copper ribbon; the number of turns in the coil winding is 55, the winding arrangement is AAZZBBXXCCYY, and current density is 3 A/mm^2. A liquid alloy (brass) crystallizes in a water-cooled sleeve that separates the melt from the inductor.

3. Mathematical model

To solve field tasks, a cylindrical coordinate system was used, and the presence of cylindrical symmetry was assumed. In this case, the system of the electromagnetic field equations can be reduced to a single equation [20]

$$-\frac{\partial}{\partial r}\left(\frac{A_\phi}{\mu r}+\frac{1}{\mu}\frac{\partial A_\phi}{\partial r}\right)-\frac{\partial}{\partial z}\left(\frac{1}{\mu}\frac{\partial A_\phi}{\partial z}\right)+\beta\frac{\partial A_\phi}{\partial z}+\alpha\cdot\left(\frac{A_\phi}{r}+\frac{\partial A_\phi}{\partial r}\right)+j\cdot\omega\cdot\gamma\cdot A_\phi=J_\phi \qquad (1)$$

Where $\beta=-\gamma\cdot w$and $\alpha=-\gamma\cdot v$; γ – medium specific electrical conductivity; v, w – components of medium motion speed along r and z axes, respectively.

Melt motion in a crystallizing ingot with cylindrical symmetry can be written as follows [20]

$$v=v^0+\Delta t\left\{-v\frac{\partial v}{\partial r}-w\frac{\partial v}{\partial z}+\frac{1}{\rho}F_r-\frac{1}{\rho}\frac{\partial P}{\partial r}+\upsilon_t\left(\frac{\partial^2 v}{\partial r^2}+\frac{\partial^2 v}{\partial z^2}+\frac{1}{r}\frac{\partial v}{\partial r}-\frac{v}{r^2}\right)\right\}; \qquad (2)$$

$$w=w^0+\Delta t\left\{-v\frac{\partial w}{\partial r}-w\frac{\partial w}{\partial z}+\frac{1}{\rho}F_z-\frac{1}{\rho}\frac{\partial P}{\partial z}+\upsilon_t\left(\frac{\partial^2 w}{\partial r^2}+\frac{\partial^2 w}{\partial z^2}+\frac{1}{r}\frac{\partial w}{\partial r}\right)\right\} \qquad (3)$$

In equations (2) and (3), F_r, F_z – components of the density of electromagnetic forces obtained in the calculation of the electromagnetic field according to equation (1); υ_t – eddy kinematic viscosity.
To solve equations (2), (3), the finite-difference method with a staggered grid was used (see, for example, [21]).

The following equation was used for determination of temperatures in a moving medium [20]

$$\frac{\partial T}{\partial t}=-v\frac{\partial T}{\partial r}-w\frac{\partial T}{\partial z}+a_t\left(\frac{\partial^2 T}{\partial r^2}+\frac{1}{r}\frac{\partial T}{\partial r}+\frac{\partial^2 T}{\partial z^2}\right)+\frac{q_V}{\rho C_p}+\frac{L}{C_p}\frac{\partial \psi}{\partial t} \qquad (4)$$

Where q_V – rate of internal heat sources; a_t – eddy diffusivity; L, ψ – crystallization heat and hard phase proportion, respectively; C_p, ρ – heat capacity and density, respectively.

4. Procedure for joint solving of field tasks

The specifics of simultaneous solving the above-mentioned tasks are their various time constants. During simulation, the following provisions have been adopted:

1) a change in the temperature and hydrodynamic fields is considered in dynamics;

2) the electromagnetic field is steady-state;

3) the hydrodynamic field is recalculated at each time interval in order to take into account the occurring solid phase in the melt;

To perform calculations, the finite-difference method was used, and an author's software package which allows for obtaining the necessary results with acceptable accuracy was created.

5. Simulation results

A fragment of the calculation area is shown in Figure 1. The liquid melt area was divided into 10 layers along the *r* axis (horizontal axis) and 56 layers along the *z* axis (vertical axis).

The melt motion speed practically does not affect the energy characteristics of the electromagnetic field, which follows from the calculations performed in the course of the study. Therefore, the electromagnetic field is calculated once.

The flow structure has a dual-vortex nature (Figure 2) with maximum speeds on the axis of symmetry (*r*= 0), which are about 0.74 m/s in the middle of the height. In the melt layer as close to the inductor as possible, the highest speed is about 0.4 m/s at the supply current frequency of 500 Hz.

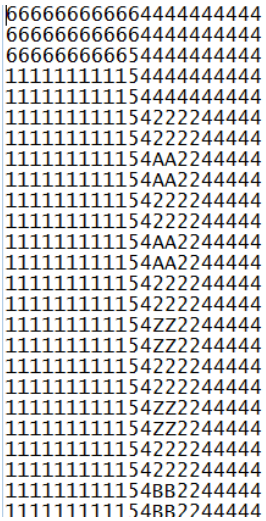

Figure 1. Fragment of the calculation area:
1 – melt area; 2 – iron circuit;
A, Z, B – phase windings; 4 – air;
5 – crystallizer; 6 – heat insulation.

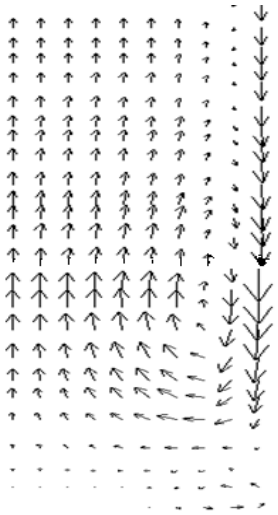

Figure 2. Fragment of the molten metal motion at the supply current frequency of 500 Hz. The field direction is from top to bottom.

The crystallization temperature range was 1,083–1,070 K. It was assumed that the initial melt temperature was 1,090 K. The melt crystallization begins about 100 s after the start of calculations. The first crystals appear in the metal layer closest to the inductor (since there is a water-cooled insert). In this layer, there is the largest temperature gradient from all areas with liquid metal.

The crystallization front moves from the metal layers closest to the inductor towards the ingot axis. It was found that the crystallization rate was in the range of 3–5 mm/min in the first 5–25 minutes after the start of simulation.

As it is known (see, for example, [1,2]), crystal growth occurs in the direction opposite to the direction of the heat flux, which in turn is determined by the temperature field gradient

$$\vec{q} = -\lambda \cdot \left(\frac{\partial T}{\partial r} \vec{e}_r + 0\vec{e}_\phi + \frac{\partial T}{\partial z} \vec{e}_z \right)$$

Let us try to establish the relationship between the temperature field gradient during crystallization and the solid metal alloy structure.

For the number of calculation steps of 540 (25 minutes), the fraction of the solid phase in each cell of the calculation area exceeds 0.75 Let us compare the experimentally observed structure of the metal

ingot and the components of the temperature gradient $\frac{\partial T}{\partial r}$. In the outer layer with a thickness of 1/10 of the ingot radius, an equiaxial fine-grain structure is observed. In the inner layer (from the center to the periphery) with a thickness of 5/10 of the ingot radius, equiaxial large crystals are observed. Between these layers (4/10 of the ingot radius), columnar crystals directed along the radius are observed. We believe that the ingot grain size is related to the crystallization rate [2]. It has been found that quantitatively, the relationship between the temperature field gradient during crystallization and the ingot structure can be expressed in the following rules:

- elongated grains of about 10 mm – cooling rate of about $1.8 \cdot 10^{-4}$ kg/s;
- elongated grains of about 20-30 mm – cooling rate of about $0.7 \cdot 10^{-4}$–$1.8 \cdot 10^{-4}$ kg/s;
- globular grains with a size of 10-20 mm – cooling rate of less than $0.7 \cdot 10^{-4}$ kg/s.

Let us apply the obtained rules for simulation of a crystallizing ingot structure.

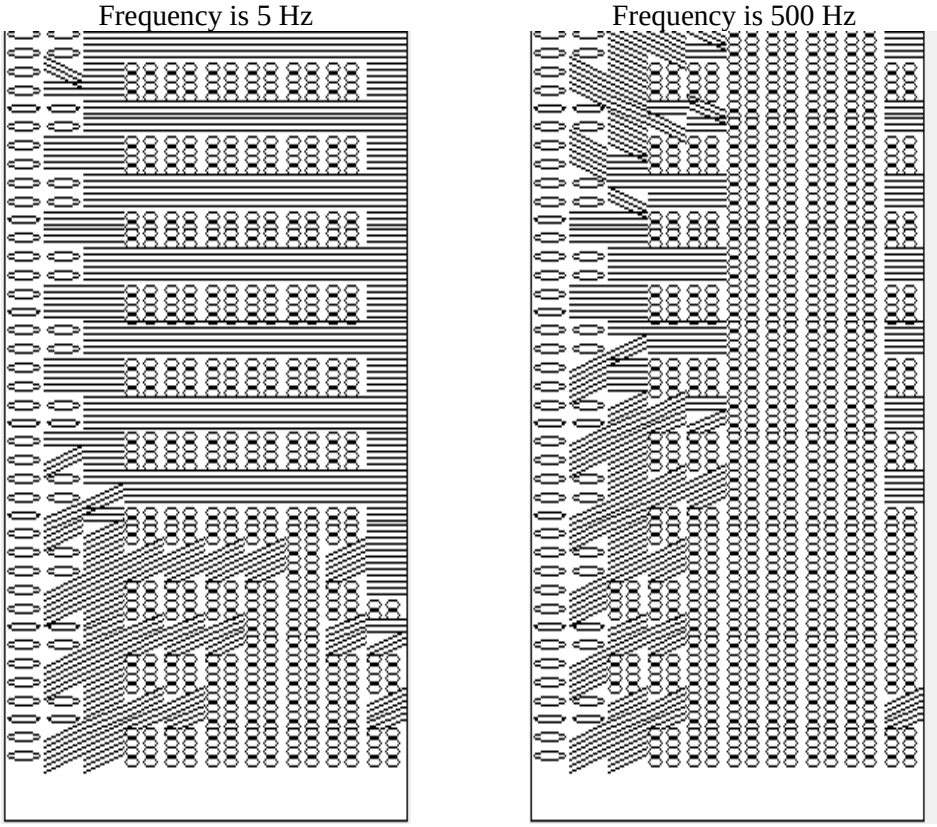

Figure 3. Result of simulation of the ingot axial section structure (a part of the ingot is shown).
– small crystals; – dendritic structure;
– large globular crystals.

Figure 3 shows the calculated structure of the crystallized ingot for two current frequencies in the inductor (*r=0* axis on the left; inductor on the right). From these results it follows that in the outer layer of the ingot, smaller elongated crystals (continuous small ellipses) form. Next to them and further to the center of the ingot, crystals in the form of dendrites (horizontal and inclined lines showing the direction of their growth) form. Then the formation of larger globular grains (large ellipses) located near the ingot axis begins.

The impact of the current frequency in the inductor is observed (Figure 3). At the frequency of 5 Hz, dendritic structures penetrate the ingot throughout the cross section. At the current with frequency of 500 Hz, a wide zone of small crystals appears and is about half the cross section. Further to the center of the ingot, there form crystals in the form of dendrites (horizontal and inclined lines). Then the formation of larger globular grains (large ellipses) located near the ingot axis begins.

6. Conclusion

- A quantitative relationship between the temperature field gradient, crystallization rate and grain size has been established.
- Molten metal crystallization in an electromagnetic field has been simulated.
- It has been shown that an increase in the current frequency from 5 to 500 Hz leads to the expansion of the area with small crystals.

References

[1] Samoilovich Yu A 1983 *System Analysis of an Ingot Crystallization* (Kiev: Naukova Dumka) [In Russian]
[2] Winegard W 1967 *An Introduction to the Solidification of Metals* (Moscow: Mir) [In Russian]
[3] Zhai L L, Ban C Y and Zhang J W 2019 Investigation on laser cladding Ni-base coating assisted by electromagnetic field *Optics & Laser Technology* **114** pp 81–8
[4] Xu Y, Wang T, Wang F and Wang E 2017 Influence of lower frequency electromagnetic field on dendritic crystal growth in special alloys *Journal of Crystal Growth* **468** pp 506–9
[5] Zhai L, Ban C, Zhang J and Yao X 2019 Characteristics of dilution and microstructure in laser cladding Ni-Cr-B-Si coating assisted by electromagnetic compound field *Materials Letters* **243** pp 195–8
[6] Chen X, Jia Y, Liao Q, Jia W, Le Q, Ning S and Yu F 2019 The simultaneous application of variable frequency ultrasonic and low frequency electromagnetic fields in semi continuous casting of AZ80 magnesium alloy *Journal of Alloys and Compounds* **774** pp 710–20
[7] Yang Y, Chen R, Guo J, Ding H and Su Y 2018 Numerical analysis for electromagnetic field Influence on heat transfer behaviors in cold crucible used for directional solidification *International Journal of Heat and Mass Transfer* **122** pp 1128–37
[8] Khatsayuk M Yu, Pervukhin M V and Golovenko Ye A 2011 MHD-Processes in the Liquid Phase of an Ingot Formed in a Magnetic Field *News of Higher Educational Institutions. Electromechanics* **1** pp 26–30
[9] Bana B, Zhang T, Lia J, Baia X, Pana X, Chena J and Tabaian S H 2018 Solidification refining of MG-Si by Al-Si alloy under rotating electromagnetic field with varying frequencies *Separation and Purification Technology* **202** pp 266–74
[10] Zoua Q, Hanb N, Shenb Z, Jiea J and Li T 2018 Effects of AlB2/AlP phase and electromagnetic stirring on impurity B/P removal in the solidification process of Al-30Si alloy *Separation and Purification Technology* **207** pp 151–7
[11] Nikitin K V, Amosov E A, Nikitin V I, Glushenkov V A and Chernikov D G 2015 Theoretical and Experimental Substantiation of Treatment of Aluminum-Based Melts by Pulsed Magnetic Fields *News of Higher Educational Institutions. Non-Ferrous Metallurgy* **5** pp 11–9
[12] Goman V, Sokolov I and Fedoreev S 2019 Modeling electromagnetic stirring processes during continuous casting of large-format slabs. *International Conference on Industrial Engineering, Applications and Manufacturing, ICIEAM 2019* (Institute of Electrical and Electronics Engineers Inc.) https://doi.org/10.1109/ICIEAM.2019.8743005
[13] Tsaplin A I 1986 Dynamics of the Circulation of a Crystallizing Continuous Ingot Liquid Core in the Traveling Field of an Inductor *Magnetic Hydrodynamics* **1** pp 127–31 [In Russian]
[14] Sarapulov F N, Sidorov O Yu and Timofeev V N 2001 Induction MHD-devices and mathematical simulation *Fifth international Conf. on Unconventional electromechanical and*

electrical systems (Miedzyzdroje, Poland, September 05-08) **1** p 165
[15] Sarapulov F N, Sarapulov S F, Sidorov O Yu and Sokunov B A 2006 Formation of Electromagnetic Impact on the Liquid Phase of a Crystallizing Ingot *Collection of Research Papers of the 12th International Ples Conference on Magnetic Fluids* (August-September, 2006. Ples, Russia. State Educational Institution of Higher Professional Education Ivanovo State Power University named after V I Lenin) p 407
[16] Gruzdeva I A, Sulitsin A V, Mysik R K and Sokunov B A 2006 Influence of Electromagnetic Stirring on the Quality of Tin Bronze Ingots *Proceedings of the International Research-to-Practice Conference. Features of Treatment and Use of Products Made of Heavy Non-Ferrous Metals* (Yekaterinburg: Ural Branch of the Russian Academy of Sciences) p 147
[17] Begalov V, Bychkov A, Sarapulov F and Sokunov B 2004 Poliphase schemes of inductors for electromagnetic treatment of smelts *Proceedings of HES-04* (Padua, Italy) p 79
[18] Erkenov N Kh 2002 Study of the Influence of Power Supply Systems on the Parameters of an Electromagnetic Crystallizer *News of Higher Educational Institutions. Electromechanics* **2** pp 28–31
[19] Sarapulov S F, Sokunov B A and Frizen V E 2003 Induction Agitator for Aluminum Alloys Stirring during Crystallization *Issue 38. Bulletin of USTU. Electromechanical and Electromagnetic Energy Converters and Controlled Electromechanical Systems: Collection of Articles. Part 2: Special Electrical Machines and Electromagnetic Devices. Energy Saving Issues. Educational Projects.* (Yekaterinburg: USTU) no 5 (25) p 171 [In Russian]
[20] Sidorov O Yu, Sarapulov F N and Sarapulov S F 2010 *Finite-Element and Finite-Difference Methods in Electromechanics and Electrotechnics* (Moscow: Energoatomizdat) [In Russian]
[21] Patankar S 1984 *Numerical Heat Transfer and Fluid Flow* (Moscow: Mir) [In Russian]